

## SYNTHESIS, CHARACTERIZATION AND ANTIBACTERIAL ACTIVITY OF SN(II) AND SN(IV) IONS COMPLEXES CONTAINING N-ALKYL-N-PHENYL DITHIOCARBAMATE LIGANDS

Wissam Abbas Ali<sup>1</sup>, Hayder Hamied Mihsen<sup>1,✉</sup>, Sajid H. Guzar<sup>2</sup>

<https://doi.org/10.23939/chcht17.04.729>

**Abstract.** In the current study, ligands S2 donor atoms, sodium *N*-methyl-*N*-phenyldithiocarbamate [L1], and sodium *N*-ethyl-*N*-phenyldithiocarbamate [L2] are prepared from carbon disulfide with *N*-methyl aniline and *N*-ethyl aniline, respectively. Sn(II) and Sn(IV) ions complexes containing *N*-alkyl-*N*-Phenyl dithiocarbamate are prepared and characterized by CHNS elemental analysis, infrared spectroscopy (FT-IR), <sup>1</sup>H NMR-spectroscopy, mass spectroscopy, UV-visible spectroscopy, magnetic susceptibility and conductivity measurements. The analytical and spectral data show that the stoichiometry for all complexes is 1 : 2 metal to ligand. The spectral data confirm good coordination of dithiocarbamate ligand with the metal through sulfur atoms of dithiocarbamate moiety. Molar conductivity of complexes are measured using DMF as a solvent and indicated that the complexes of Sn(II) are non-ionic whereas Sn(IV) complexes are ionic. The ligands L1 and L2 and their complexes are examined against *Staphylococcus aureus* bacteria and *Escherichia coli* bacteria.

**Keywords:** antibacterial activity, N-alkyl-N-phenyl dithiocarbamate, tin complexes, spectral data.

### 1. Introduction

Carbamate DTCs analogs and amide of dithiocarbamic acid (DTCs) are described as "versatile ligands"; however, this is considered as an understatement because of their ability to form stable complexes with a wide range of primary and transition metals.<sup>1</sup> They can be used for various types of chemicals and situations. Also, their attachment to other molecules is possible with dithiocarbamates,<sup>2</sup> because they have two sulfur atoms, which are continually ready to contribute their electrons

to the metal atom centers in at least nine distinct coordination modes. As a result, a wide range of binding characteristics can be obtained. Dithiocarbamates are used to bond together almost identical metallic-sulfur linkages. DTC derivatives are widely used as herbicides, pesticides, antibacterial, antifungal, and anticancer medicines.<sup>3,4</sup> Bacterial growth can be slowed by interfering with the metabolic functions of the bacterium. For food and turf disease prevention (thiram),<sup>5,6</sup> and for alcoholism treatment (disulfiram), several DTC derivatives are currently in use. In addition, dithiocarbamate metal complexes have been found to be useful precursors for metal sulfide nanoparticles.<sup>7,8</sup>

These metalloids include the tin(II), and tin(IV) isomers. Moreover, structural diversity, catalytic and redox capacity, ability to interchange ligands, and a wide spectrum of interactions with therapeutic effects<sup>9</sup> are some of the unique chemical aspects of these compounds. At least one carbon-tin bond has been identified to have an impact on the overall activity of the molecule. Sn atom activity is also affected by the amount and type of alkyl/aryl (R) substituents attached to it. Tin(II), (IV) different properties have been shown to be significantly influenced by variations in the alkyl or aryl group substituents.<sup>10,11</sup> Yet, the mechanism by which tin(II) and tin(IV) compounds exert their therapeutic actions on tumor cells has not been established. Antibacterial, anti-cancer, schizonticidal, antimalarial, and biocidal properties have been demonstrated in agriculture.<sup>12,13</sup> Complexes of tin(II), and tin(IV) cations may be formed by the ligands containing the donor atoms S, N, O, and P. Dithiocarbamate is one of these ligands.<sup>12</sup>

Tin (II),(IV) dithiocarbamate complexes have been used as anti-cancer drugs,<sup>13</sup> antibacterial agents, catalysts for the synthesis of other compounds,<sup>14</sup> SnS nanoparticles, or a single-source precursor.<sup>15</sup> Researchers found that the complexes either evaporate, leaving behind a little quantity of residue, or decompose and produce the equivalent metal sulfide.<sup>16</sup> When compared to other structurally related compounds, tin dithiocarbamates show complex thermochemistry and an unusual

<sup>1</sup> Chemistry Department, College of Science, Kerbala University, Iraq

<sup>2</sup> Chemistry Department, College of Education for Pure Sciences, Kerbala University, Iraq

✉ hayder.kandoh@uokerbala.edu.iq, hayderalhmedawy@gmail.com

© Ali W.A., Mihsen H.H., Guzar S.H., 2023

pattern of heat breakdown. Consequently, certain tin(II),(IV) complexes of *N*-methyl or *N*-ethyl -*N*-phenyl dithiocarbamates are produced and described in this study.

## 2. Experimental

### 2.1. Chemicals and Instrument

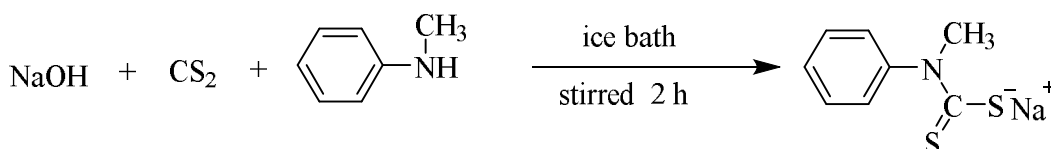
In the current study, sodium hydroxide 97% (GCC, England), carbon disulfide 99.8 (LOBA. Chem), *N*-methyl aniline 89% (GCC, England), *N*-ethyl aniline 99% (Merk, KGaA, Germany), Diethyl ether 95% (Scharlau), Ethanol 99% (Sigma-Aldrich, Germany), Tin(II) chloride dihydrate 99% (BDH, England), Tin(IV) chloride pentahydrate 98% (BDH, England) were used. On the other hand, the methods utilized in this project are innovative. FT-IR spectra of the ligands L1 and L2 and their complexes were characterized using the FTIR 8400s (Shimadzu). The spectra were recorded in the range of 4000-400 cm<sup>-1</sup>. NMR spectra were obtained by a BAMX400 MHZ Spectrophotometer in DMSO-d<sub>6</sub> as a solvent. UV-visible spectra were reordered using Shimadzu double beam 1800 UV spectrophotometer in dimethylformamide (DMF) as a solvent at 1x10<sup>-3</sup> M. Elemental analyses were performed

by using a EuroEA Elemental Analyzer. The melting point of compounds produced was measured by using the Gallen Kamp melting point. The molar conductivity for complexes was measured using Digital Conductivity Series. The magnetic susceptibility of prepared complexes was measured by using a magnetic susceptibility balance, Johnson Matthey.

### 2.2. Synthesis of Sodium

#### N-methyl-N-phenyldithiocarbamate [L1]

Sodium hydroxide (2 g, 0.05 mol) was dissolved in a small amount (approximately 3 mL) of distilled water and allowed to cool. To this cold solution, a carbon disulfide (3.8 g, 0.05 mol) was added. *N*-methyl aniline was then added (5.44 mL, 0.05 mol). The mixture was swirled for 2 hours at a temperature below 4 degrees Celsius. The result was a yellowish-white solid product that was separated, filtered, washed with ether, and then recrystallized with warm acetone. The white solid product was dried under vacuum over CaCl<sub>2</sub> at room temperature giving 1.633 g (yield = 82%) of the product with mp > 300 °C.<sup>17</sup> Elemental analysis CHNS: Found (%): C; 46.80 ; H; 3.91 ; N; 6.80 ; S; 31.22. Calc. C; 46.82; H; 3.92; N; 6.82; S; 31.24. The general steps of preparation are shown in Scheme 1.



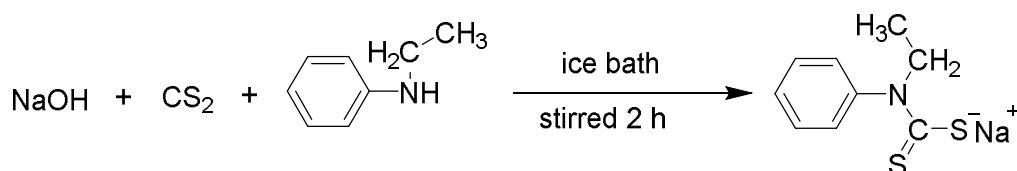
**Scheme 1.** Schematic representation for the preparation of Sodium *N*-methyl- *N*-phenyldithiocarbamate [L1]

### 2.3. Synthesis of Sodium

#### N-ethyl-N-phenyldithiocarbamate [L2]

Sodium hydroxide (2 g, 0.05 mol) was dissolved in a minimum amount (about 3 mL) of distilled water and allowed to attain an ice temperature. To this cold solution a carbon disulfide (3.8, 0.05 mol) was added. This was followed by the addition of *N*-ethyl aniline (6.05 mL, 0.05 mol). The mixture was stirred for 2 hrs while keeping

the temperature below 4 °C. A yellowish-white solid product was formed, separated, filtered, washed with ether, and finally recrystallized with warm acetone. The white solid product was dried under vacuum over CaCl<sub>2</sub> at room temperature giving 0.42 g (yield = 51%) of the product with a melting point of 215 °C.<sup>17</sup> The elemental analysis CHNS: Found (calc.) %: C; 49.27 (49.29); H; 4.56 (4.59); N; 6.37 (6.38); S; 29.20 (29.23) . The general steps of preparation are shown in Scheme 2.



**Scheme 2.** Schematic representation for the preparation of Sodium *N*-ethyl- *N*-phenyldithiocarbamate [L2]

**Table 1.** Physical properties of tin complexes

Complex	Metal ion	Yield%	Color	Melting point °C (de)
C1L1	Sn(II)	75	Yellowish-white	350
C2L1	Sn(IV)	76	Yellowish-white	350
C3L2	Sn(II)	78	Yellowish-white	330
C4L2	Sn(IV)	70	Greenish-yellow	265

## 2.4. Synthesis of the Tin Complexes with L1 and L2 Ligands

To a stirred solution of appropriate ligand (2 mol) in ethanol (5 mL), a solution of tin chloride (1 mole) in 5 mL of ethanol was added. The mixture was refluxed for about 1 hr. The colored precipitate was filtered, washed with ethanol and dried under vacuum. The physical properties of the synthesis complexes are shown in Table 1.

## 3. Results and Discussion

### 3.1. Infrared Spectroscopy

Figs. (1-2) and Table 2 show FT-IR peaks of ligands L1 and L2. They are 3367, 3351  $\text{cm}^{-1}$ , and 1633, 1627  $\text{cm}^{-1}$ , respectively, characterized by O-H stretching and vibrational bands of water. This indicates that the compounds are hydrated. Some alkali salts of dithiocarbamate are known to be crystallized with lattice water molecules.<sup>17,18</sup> The "thioureide" bands (-N-C(=S)) of ligands L1 and L2 were observed as sharp peaks at 1442 and 1438  $\text{cm}^{-1}$ , respectively.<sup>19</sup> The stretching frequencies of  $\nu(\text{C}_2\text{-N})$  groups were observed within the range of 1250–1350  $\text{cm}^{-1}$ .<sup>20</sup> The emergence of a new peak  $\nu_{\text{asym}}(\text{C}=\text{S})$  of sodium salts of dithiocarbamates was obser-

ved for ligands L1 and L2, which occurred at 962  $\text{cm}^{-1}$  and 987  $\text{cm}^{-1}$ , respectively, with disappearance of the stretching vibrations N-H for the *N*-methyl aniline molecule.<sup>21</sup> The FT-IR spectra of tin (II) complexes (C1L1) and (C3L2), are shown in Figs. (3-4) and Table 2. In the FT-IR spectra of the complexes, a strong thioureide  $\nu(\text{C}-\text{N})$  band of (C1L1) and (C3L2) complexes was found in the region of 1491  $\text{cm}^{-1}$  and 1485  $\text{cm}^{-1}$  respectively.<sup>22</sup> The high stretching vibration can be ascribed to an increase in the carbon-nitrogen double bond character due to the delocalization of electrons toward the metal atom in each complex. Split absorption bands of  $\nu(\text{C}-\text{S})$  stretching vibrations in (C1L1) and (C3L2) complexes were observed in the range of 1070–1068  $\text{cm}^{-1}$ , which indicated a bidentate mode of coordination through the sulfur atom of the dithiocarbamate moiety.<sup>22</sup> The  $\nu(\text{Sn}-\text{S})$  bands (found in the far-infrared region) were observed around 411–450  $\text{cm}^{-1}$ . This band indicates coordination between the tin ion and the ligand moiety. Tin (IV) complexes (C2L1) and (C4L2) spectra are shown in Figs. (5-6) and Table 2. In the FT-IR spectra of these complexes, a strong thioureide  $\nu(\text{C}-\text{N})$  band was found in the region of 1489  $\text{cm}^{-1}$ , 1485  $\text{cm}^{-1}$ , respectively.<sup>23</sup> A sharp band assigned to the  $\nu_{\text{asym}}(\text{C}-\text{S})$  stretching is observed at 1097 and 1093  $\text{cm}^{-1}$  for (C2L1) and (C4L2), respectively. The  $\nu(\text{Sn}-\text{S})$  bands (found in the far-infrared region) were observed around 411–459  $\text{cm}^{-1}$ . This band indicates coordination between the tin compounds and the ligand moiety.

**Table 2.** FT-IR Spectra data for ligands and Complexes

Compound	C-H (Methyl or ethyl)	C-N thioureide	C=S	C-S	M-S
L1	2825, 2937	1442	960	1158	–
(C1L1)	2850, 2920	1491	1016	1070	445
(C2L1)	2833, 2933	1489	1014	1097	437
L2	2982	1438	987	1158	–
(C3L2)	2980	1485	1001	1068	435
(C4L2)	2983	1485	1031	1093	459

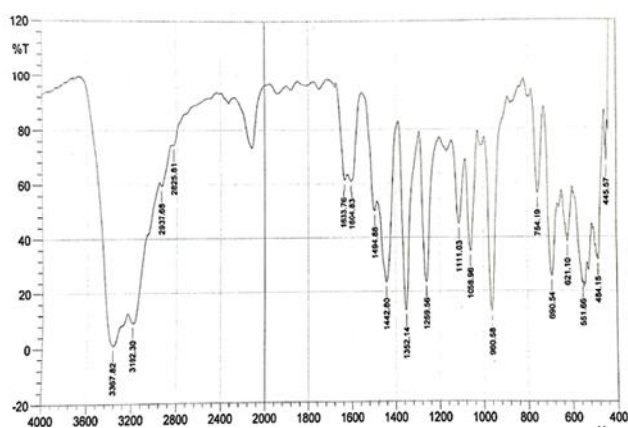


Fig. 1. FT-IR spectrum of Ligand L1

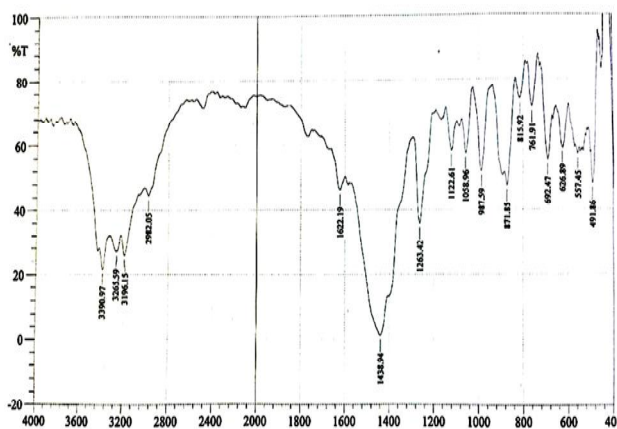


Fig. 2. FT-IR spectrum of Ligand L2

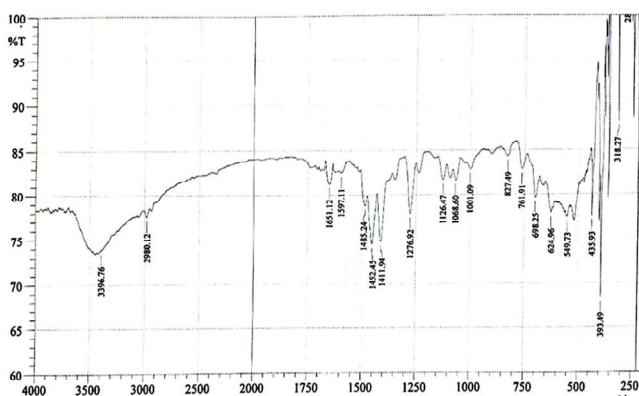


Fig. 4. FT-IR spectrum of Complex (C3L2)

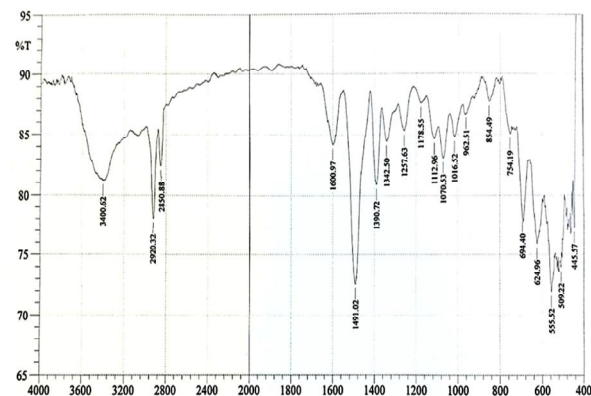


Fig. 3. FT-IR spectrum of Complex (C1L1)

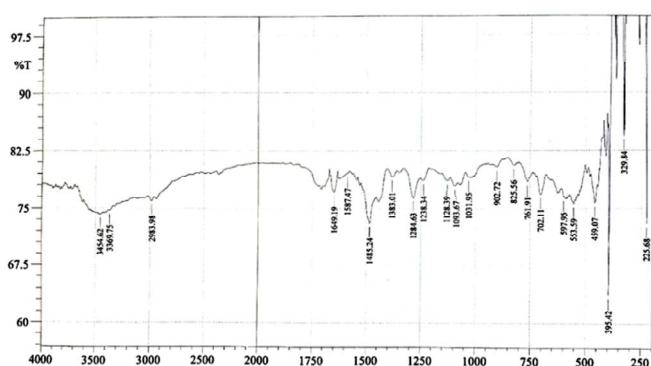


Fig. 6. FT-IR spectrum of Complex (C4L2)

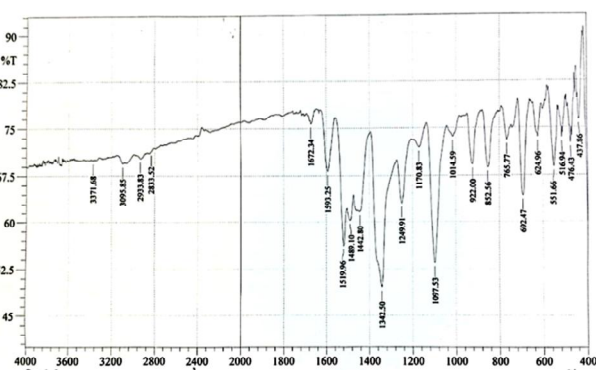


Fig. 5. FT-IR spectrum of Complex (C2L1)

### 3.2. $^1\text{H}$ NMR and mass Spectroscopy of Complexes

In  $^1\text{H}$  NMR spectra of (C1L1) and (C2L1) complexes (Figs. 7-8) a singlet peak at  $\delta=3.25$  ppm is observed, equivalent to three protons of the methyl group

in  $\text{N}-\text{CH}_3$ , as well as at  $\delta=(7.20-7.60)$  ppm, attributed to the aromatic protons.  $^1\text{H}$  NMR spectra of (C3L2) and (C4L2) complexes are shown in Figs. 9-10. The methyl group and the methylene group of the ethyl substituents appear between 1.25–1.30 ppm as a triplet, and between 3.05–3.15 ppm as a quartet, respectively, and at  $\delta=(7.20-7.57)$  ppm, attributed to the aromatic protons.<sup>12, 24-26</sup>

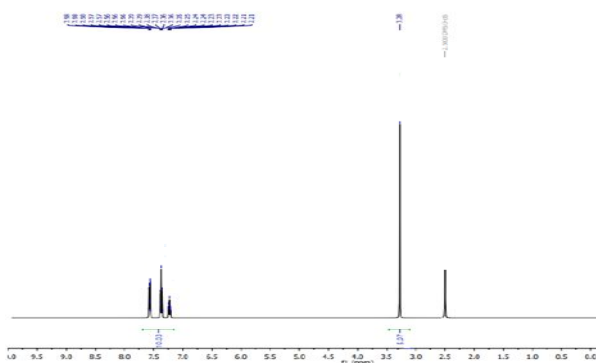


Fig. 7. <sup>1</sup>H NMR Spectrum of Tin(II) Complex (C1L1)

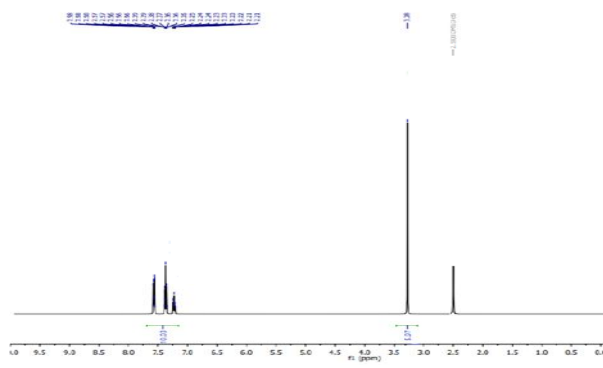


Fig. 8. <sup>1</sup>H NMR Spectrum of Tin(IV) Complex (C2L1)

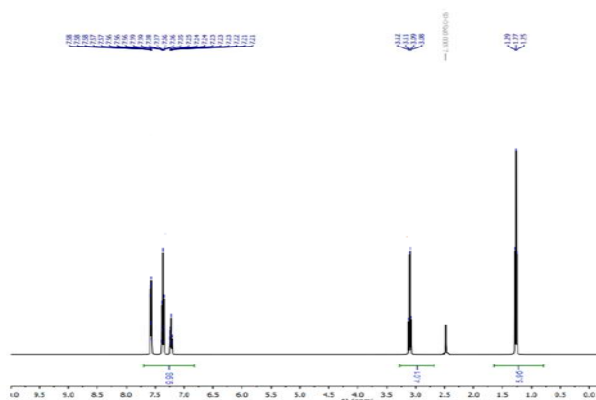


Fig. 9. <sup>1</sup>H NMR Spectrum of Tin(II) Complex (C3L2)

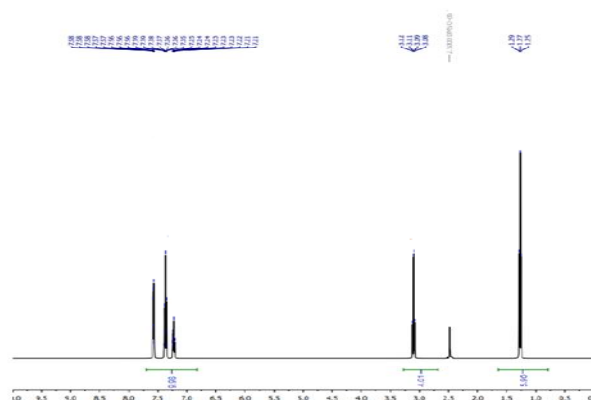


Fig. 10. <sup>1</sup>H NMR Spectrum of Tin(IV) Complex (C4L2)

The mass spectra of the complexes (C1L1), (C2L1), (C3L2), and (C4L2) were recorded to establish their structural formula, as illustrated in Figs. 11-14. The experimental parent molecular ion peaks of prepared complexes were at (483.20), (554.10), (511.90), and (581.70) (m/z), whereas the theoretical ones were (483.27), (554.17), (511.95) and (581.67), respectively. The results are consistent with the proposed molecular formula of each compound. The most significant ligands are thioureide and thiocarbonyl coupled with the production of positive molecular ions and other positively charged fractions.

### 3.3. Electronic Spectra and Magnetic Properties

Two kinds of transitions may be seen in the electronic spectrum of the ligand (L1), ( $\pi \rightarrow \pi^*$ ) and ( $n \rightarrow \pi^*$ ) Fig. 15. The transitions with a ( $\pi \rightarrow \pi^*$ ) are more powerful than those with ( $n \rightarrow \pi^*$ ). The peaks were observed at 251 nm, which corresponds to the electronic transmission ( $\pi \rightarrow \pi^*$ ) in pi system in a benzene ring and N=C=S systems, and at 321 nm, which corresponds to the electronic transmission ( $n \rightarrow \pi^*$ ) in nitrogen and sulfur sys-

tems ( $n \rightarrow \pi^*$ ).<sup>27-30</sup> The electronic spectra of complexes (C1L1) and (C2L1), showed the same bands at 294 nm, 364 nm, 492 nm (Figs. 16-17), but the difference is in the strength of the bands. The bands around 294 nm are intra-ligand bands due to ( $\pi - \pi^*$ ) transition and those bands around 364 nm are also intra-ligand bands due to ( $n \rightarrow \pi^*$ ) transitions. For Sn(II) complexes with electronic configuration  $d^{10}$ , no d-d transitions were expected; however, the bands observed in the visible region at 492 nm of the complexes were metal to ligand charge transfer (MLCT) bands, consistent with a  $d^{10}$  system that tailed into the visible region. This confirms the existence of the tetrahedral geometry in the (C1L1) and (C2L1) complexes.<sup>31</sup> The electronic spectrum of the ligand L2 (Fig. 18), shows two electronic bands, which are assigned to the ( $\pi \rightarrow \pi^*$ ) transitions in pi system in the benzene ring and N=C=S system, and ( $n \rightarrow \pi^*$ ) transition located on the nitrogen and sulfur atoms. The peaks were observed at 254 nm, which corresponds to the pi system in the benzene ring and N=C=S system's ( $\pi \rightarrow \pi^*$ ) electronic transmission, and at 317 nm, which corresponds to the nitrogen and sulfur system's ( $n \rightarrow \pi^*$ ) electronic transmission.<sup>32,33</sup>

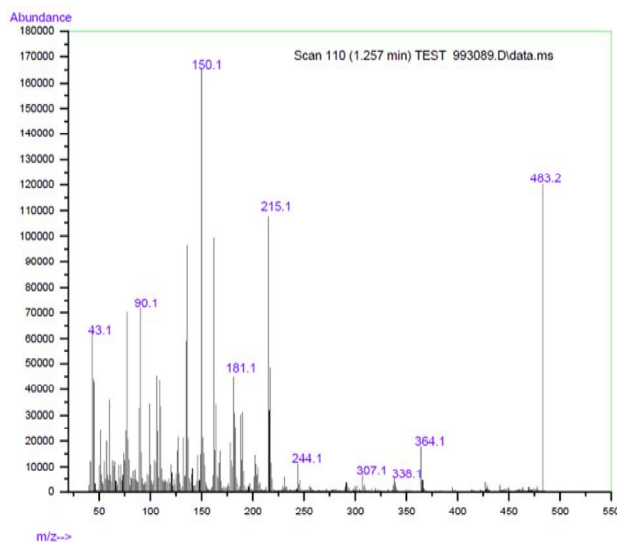


Fig. 11. Mass spectrum of Tin(II) complex (C1L1)

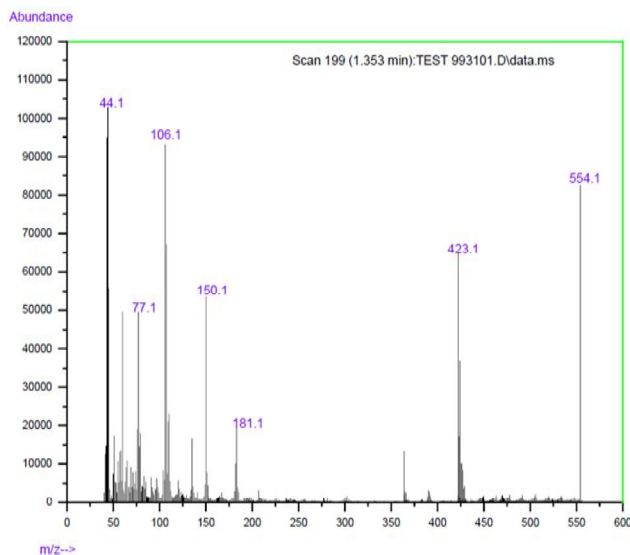


Fig. 12. Mass spectrum of Tin(IV) complex (C2L1)

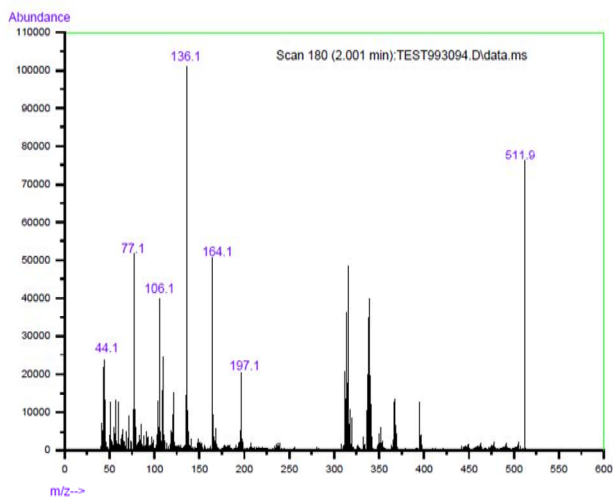


Fig. 13. Mass Spectrum of Tin(II) Complex (C3L2)

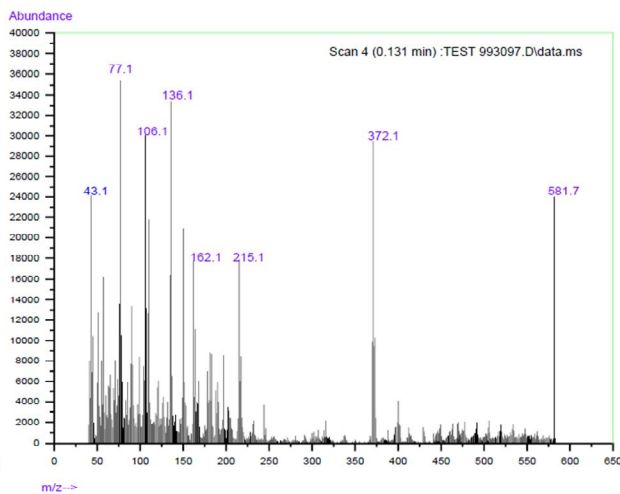


Fig. 14. Mass Spectrum of Tin(IV) Complex (C4L2)

The electronic spectra Figs. (19-20) of complexes (C3L2) and (C4L2) show the absorption peak at 281 nm, due to the ( $\pi \rightarrow \pi^*$ ) electronic transition in the pi system in the benzene ring and N-C=S group, whereas the absorption peak at 345 nm is due to the ( $n \rightarrow \pi^*$ ) electronic transition located on the nitrogen and sulfur atoms. No d-d transitions appeared in (C3L2) and (C4L2) complexes; nevertheless, bands found in the visible area of the complexes at 492 nm were metal to ligand charge transfer (MLCT) bands, consistent with a  $d^{10}$  system that tailed into the visible region. The presence of the tetrahedral geometry in the Tin(II) and (IV) complexes was thus established. This is consistent with the spectra of tetrahedral Tin(II) and (IV) complexes.<sup>32,34</sup> The magnetic susceptibility of complexes was equal to (0.0) B.M. The molar conductivity of Tin (II) complexes for the ligands L1 and L2 was measured by DMF. They were non-electrolyte and they were ( $15, 17, \text{ohm}^{-1} \cdot \text{cm}^2 \cdot \text{mol}^{-1}$ ). Tin

(IV) complexes for the ligands L1 and L2 were ( $154, 165 \text{ ohm}^{-1} \cdot \text{cm}^2 \cdot \text{mol}^{-1}$ ), respectively. These values indicated that the Tin (IV) complexes were electrolytic with 1 : 2 ratio.<sup>35</sup> The proposed structure of Sn(II),(IV) complexes is shown in Figs. 21 and 22.

### 3.4. The Effect of pH on (L1) and (L2) Ligands, Formation of Tin (II) and (IV) Complexes, and Determination of Complexes Stoichiometry

The effect of pH on L1 and L2 and their complexes were scanned. The results of (Figs. 23-28) show that the pH  $\lambda_{\text{max}}$  for the L1 and L2 was at pH=9, whereas the  $\lambda_{\text{max}}$  of their complexes was at pH=2 for (C1L1) and (C3L2), and at pH=4 for (C2L1) and (C4L2).

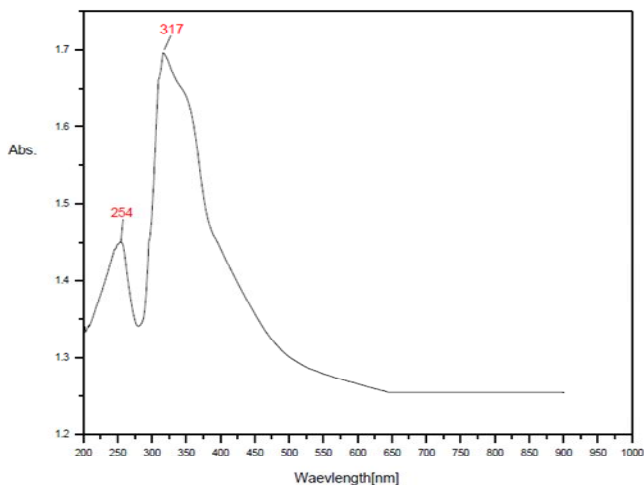


Fig. 18. UV-Vis- spectrum of ligand (L2)

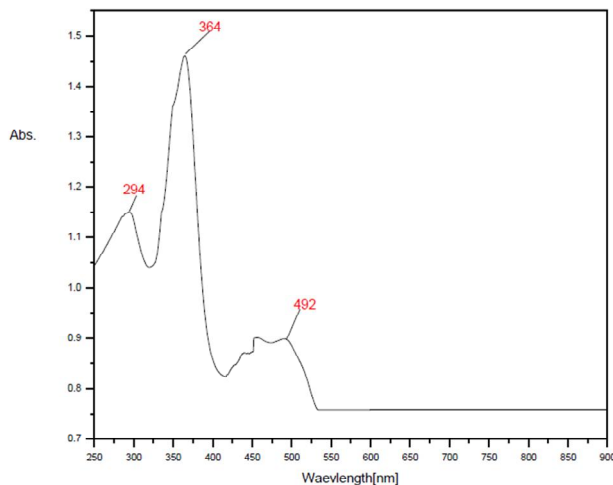


Fig. 17. UV-Vis- spectrum of Complex (C2L1)

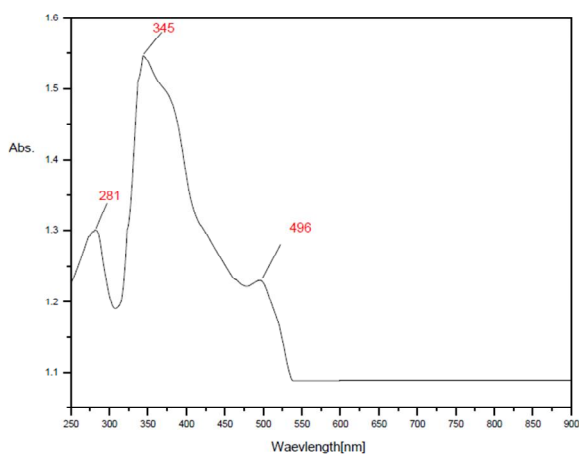


Fig. 19. UV-Vis- spectrum of Complex (C3L2)

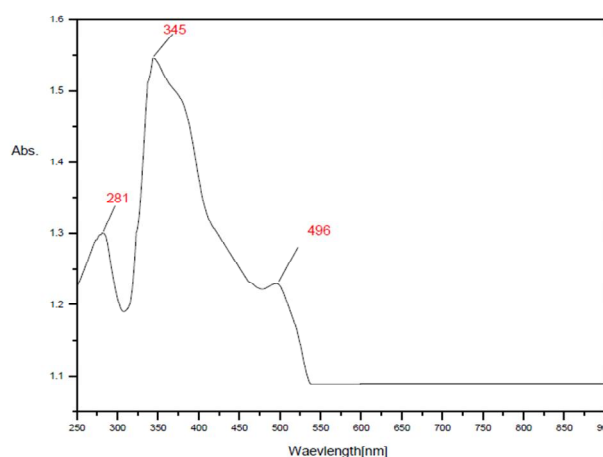
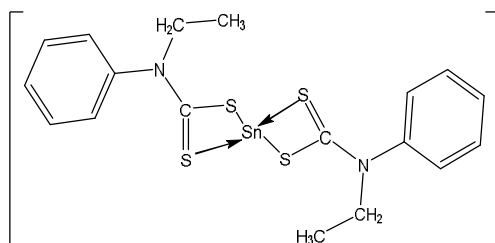
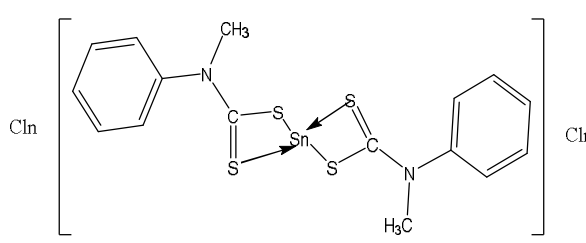


Fig. 20. UV-Vis- spectrum of Complex (C4L2)



n=0 for C3L2, n=2 for C4L2

Fig. 22. The proposed structure of (C3L2) and (C4L2) Complexes with L2 ligand



n=0 for C1L1, n=2 for C2L1

Fig. 21. The proposed structure of (C1L1) and (C2L1) Complexes with L2 ligand



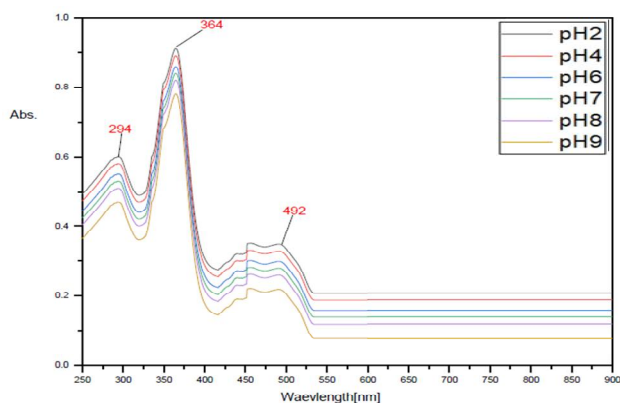


Fig. 24. pH formation of (C1L1) complex

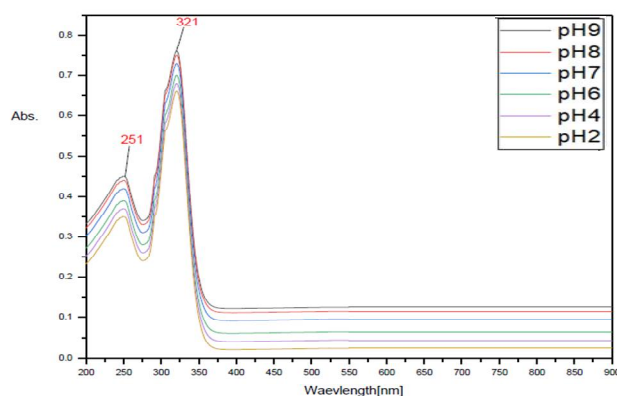


Fig. 23. pH formation of (L1) ligand

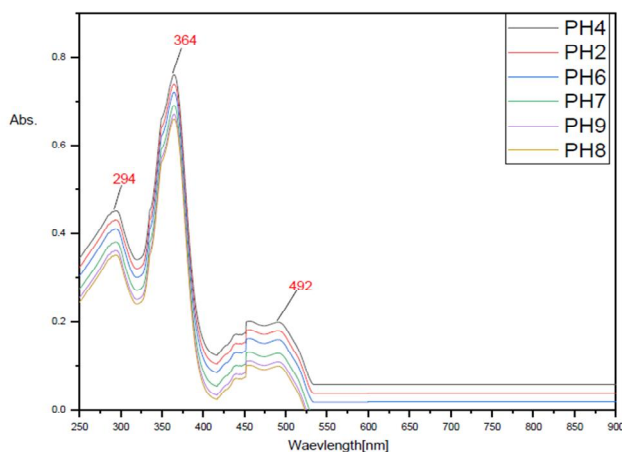


Fig. 25. pH formation of (C2L1) complex

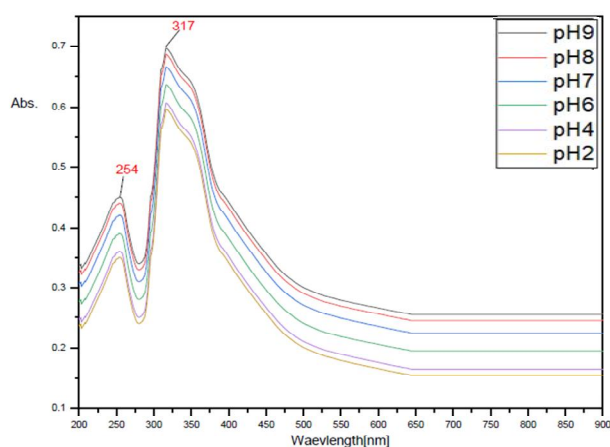


Fig. 26. pH formation of (L2) ligand

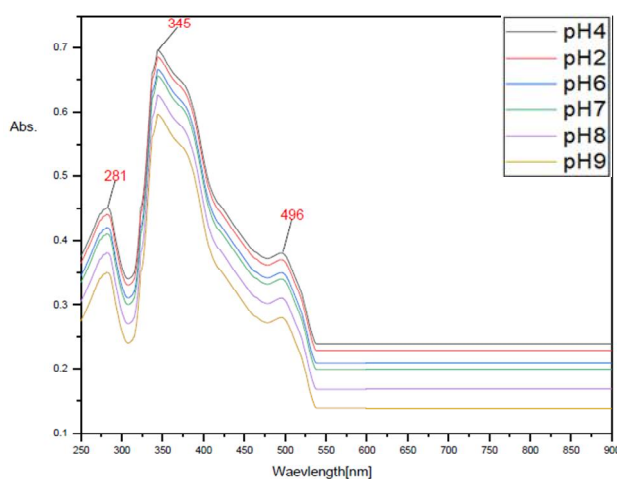


Fig. 28. pH formation of (C4L2) complex

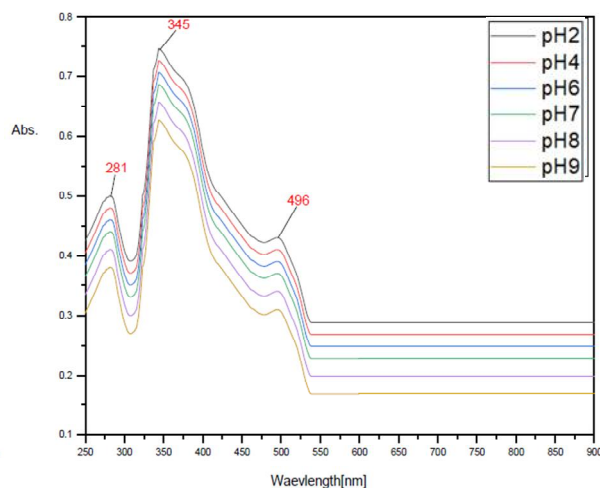


Fig. 27. pH formation of (C2L2) complex

Job's method was adopted for continuous changes in order to determine the positional formula of the complexes. This was conducted by mixing different volumes of solutions with equal concentrations ( $2.29 \times 10^{-4}$ ) of an appropriate metal ion with the L1 and L2 ligands separately to have a final volume of 10 mL. By fixing the optimum conditions

reached in this study, the absorption of the complexes was measured at the greatest wavelength  $\lambda_{\max}$ . Table 3 illustrated the results of this method. Through these results, the correlation in the complexes between the ion and the ligand ratio was (1 ; 2) mole for each one mole of metal to two moles of the ligand, *i.e.*  $ML_2$ .



**Table 3.** The results of Job's method (Continuous variables) for complexes derivative from L1, and L2 ligands at the greatest wavelength ( $\lambda_{\max}$ )

$\frac{VM}{VM + VL}$	Absorbance			
	C1L1	C2L1	C3L2	C4L2
0.1	0.115	0.115	0.226	0.332
0.2	0.275	0.284	0.295	0.416
0.3	0.486	0.491	0.478	0.592
0.4	0.490	0.486	0.494	0.595
0.5	0.468	0.471	0.467	0.582
0.6	0.448	0.456	0.456	0.562
0.7	0.437	0.442	0.425	0.541
0.8	0.325	0.430	0.423	0.521
0.9	0.416	0.419	0.420	0.510

### 3.5. Antibacterial Activity

The antibacterial activity of L1, L2 ligands, C1L1, C2L1, C3L2 and C4L2 complexes are shown in Table 4. All complexes were examined for their antibacterial activity in vitro against one type of Gram-positive bacteria (*Staphylococcus aureus*) and one type of Gram-negative bacteria (*Escherichia coli*). The agar plates were surface-inoculated uniformly from both cultures of the tested bacteria. In the solidified medium, the spaced-apart holes were all made 6 mm in diameter. These holes were filled with 40  $\mu$ L of the prepared compounds (0.01 and 0.1) g/mL in DMF as a solvent. It is worth noting that the Augmentin was used as a control drug for comparison in the same concentrations as used for the com-

plexes. These plates were incubated at 37 °C for 24 h. for both bacteria. The zones of bacterial growth inhibition around the discs were measured in (mm). The results indicated an inhibition of antibacterial activity. The L1 and L2 ligands and complexes C1L1, C2L1 and C3L2 showed greater activity against *Staphylococcus aureus* and *Escherichia coli* in high concentration, while C4L2 complex demonstrated higher activity toward *Staphylococcus aureus* and lower activity toward *Escherichia coli* in high concentration. These activities may be explained by Tweedy's chelation theory<sup>36</sup> according to which chelation reduces the polarity of the metal atom mainly because of the partial sharing of its positive charge in the ligand, which favors the permeation of the complexes through the lipid layer of the cell membrane.<sup>37</sup>

**Table 4.** The antibacterial activity of L1, L2 ligands, C1L1, C2L1, C3L2 and C4L2 complexes and Augmentin as a control drug

Bacteria	<i>Staphylococcus aureus</i>		<i>Escherichia coli</i>	
	Diameter of inhibition zone in (mm)			
	1mg	10mg	1mg	10mg
L1	12	16	11	15
L2	11	17	10	16
C1L1	13	18	14	14
C2L1	11	17	12	15
C3L2	11	12	10	14
C4L2	8	19	0	10
DMF	0	0	0	0
Augmentin	15	20	15	20

## 4. Conclusions

*N*-Alkyl-*N*-phenyl dithiocarbamate ligands L1 and L2 were used to prepare C1L1, C2L1, C3L2 and C4L2 complexes. According to elemental analyses (CHNS), <sup>1</sup>H NMR spectra, mass spectra, FT-IR spectra, UV-Vis spectra, molar conductivity and magnetic susceptibility, the structural formulas of the complexes were proposed. From

the <sup>1</sup>H NMR and FT-IR spectra, it was clear that the groups of alkyl and thioureide in the ligands changed through coordination process with tin ions. The results of mass spectra showed consistency with the theoretical molecular weights of prepared complexes with the proposed molecular formula. The molar conductance values of the complexes C1L1 and C3L2 indicate the non-electrolyte nature, and of the complexes C2L1 and C4L2

indicate 1 : 2 electrolytic nature. The antibacterial activity of the metal complexes reveals that all the prepared metal complexes have effects on *Staphylococcus aureus* and *Escherichia coli* bacteria.

## Acknowledgments

The authors are thankful to the Head of the Department of Chemistry, College of Science, University of Kerbala, Iraq for providing the necessary facilities to carry out this research.

## References

- [1] Kumar, D.N. Molecular Structure Study of Thio Schiff Base Complexes of Organotin (IV): Synthesis, Spectroscopic and Thermal Methods. *J. Mol. Struct.* **2021**, *1227*, 129569. <https://doi.org/10.1016/j.molstruc.2020.129569>
- [2] Stasevych, M.; Zvarych, V.; Khomyak, S.; Lunin, V.; Kopak, N.; Novikov, V.; Vovk, M. Proton-Initiated Conversion of Dithiocarbamates of 9,10-Anthracenedione. *Chem. Chem. Technol.* **2018**, *12*, 300–304. <https://doi.org/10.23939/chcht12.03.300>
- [3] Lee, S.M.; Heard, P.J.; Tiekink, E.R.T. Molecular and Supramolecular Chemistry of Mono- and Di-Selenium Analogues of Metal Dithiocarbamates. *Coord. Chem. Rev.* **2018**, *375*, 410–423. <https://doi.org/10.1016/j.ccr.2018.03.001>
- [4] Khan, N.; Farina, Y.; Mun, L.K.; Rajab, N.F.; Awang, N. Syntheses, Characterization, X-ray Diffraction Studies and *in vitro* Antitumor Activities of Diorganotin(IV) Derivatives of Bis(p-Substituted-N-Methylbenzylaminedithiocarbamates). *Polyhedron* **2015**, *85*, 754–760. <http://dx.doi.org/10.1016/j.poly.2014.08.063>
- [5] Landini, P.; Antoniani, D.; Burgess, J.G.; Nijland, R. Molecular Mechanisms of Compounds Affecting Bacterial Biofilm Formation and Dispersal. *Appl. Microbiol. Biotechnol.* **2010**, *86*, 813–823. <https://doi.org/10.1007/s00253-010-2468-8>
- [6] Sedlacek, J.; Martins, L.M.; Danek, P.; Pombeiro, A.J.L.; Cvek, B. Diethyldithiocarbamate Complexes with Metals Used as Food Supplements Show Different Effects in Cancer Cells. *J. Appl. Biomed.* **2014**, *12*, 301–308. <http://dx.doi.org/10.1016/j.jab.2014.04.002>
- [7] Menezes, D.C.; De Lima, G.M.; Porto, A.O.; Donnici, C.L.; Ardisson, J.D.; Doriguetto, A.C.; Ellena, J. Synthesis, Characterisation and Thermal Decomposition of Tin(IV) Dithiocarbamate Derivatives - Single Source Precursors for Tin Sulfide Powders. *Polyhedron* **2004**, *23*, 2103–2109. <https://doi.org/10.1016/j.poly.2004.06.007>
- [8] Ronconi, L.; Sadler, P.J. Applications of Heteronuclear NMR Spectroscopy in Biological and Medicinal Inorganic Chemistry. *Coord. Chem. Rev.* **2008**, *252*, 2239–2277. <https://doi.org/10.1016/j.ccr.2008.01.016>
- [9] Gasser, G.; Metzler-Nolte, N. The Potential of Organometallic Complexes in Medicinal Chemistry. *Curr. Opin. Chem. Biol.* **2012**, *16*, 84–91. <https://doi.org/10.1016/j.cbpa.2012.01.013>
- [10] Pellerito, C.; Nagy, L.; Pellerito, L.; Szorcik, A. Biological Activity Studies on Organotin(IV)<sup>++</sup> Complexes and Parent Compounds. *J. Organomet. Chem.* **2006**, *691*, 1733–1747. <https://doi.org/10.1016/j.jorganchem.2005.12.025>
- [11] Alama, A.; Tasso, B.; Novelli, F. Organometallic Compounds in Oncology: Implications of Novel Organotin as Antitumor Agents. *Drug Discov. Today* **2009**, *14*, 508–500. <https://doi.org/10.1016/j.drudis.2009.02.002>
- [12] Onwudiwe, D.C.; Nthwane, Y.B.; Ekennia, A.C.; Hosten, E. Synthesis, Characterization and Antimicrobial Properties of Some Mixed Ligand Complexes of Zn(II) Dithiocarbamate with Different N-donor Ligands. *Inorganica Chim. Acta* **2016**, *447*, 134–141. <https://doi.org/10.1016/j.ica.2016.03.033>
- [13] Javed, F.; Sirajuddin, M.; Ali, S.; Khalid, N.; Tahir, M.N.; Shah, N.A.; Rasheed, Z.; Khan, M.R. Organotin(IV) Derivatives of *o*-Isobutyl Carbonodithioate: Synthesis, Spectroscopic Characterization, X-ray Structure, HOMO/LUMO and *in vitro* Biological Activities. *Polyhedron* **2016**, *104*, 80–90. <https://doi.org/10.1016/j.poly.2015.11.041>
- [14] Tian, L.; Liu, X.; Zheng, X.; Sun, Y. Synthesis, Characterization and Cytotoxic Activity of New Diorganotin(IV) Complexes of N-(3,5-dibromosalicylidene)Tryptophane. *Appl. Organomet. Chem.* **2011**, *25*, 298–304. <https://doi.org/10.1002/aoc.1758>
- [15] Mostafa, A.M.; Mwafy, E.A.; Hasanin, M.S. One-Pot Synthesis of Nanostructured CdS, CuS, and SnS by Pulsed Laser Ablation in Liquid Environment and Their Antimicrobial Activity. *Opt. Laser Technol.* **2020**, *121*, 105824. <https://doi.org/10.1016/j.optlastec.2019.105824>
- [16] Ramasamy, K.; Kuznetsov, V.L.; Gopal, K.; Malik, M.A.; Raftery, J.; Edwards, P.P.; O'Brien, P. Organotin Dithiocarbamates: Single-Source Precursors for Tin Sulfide Thin Films by Aerosol-Assisted Chemical Vapor Deposition (AACVD). *Chem. Mater.* **2013**, *25*, 266–276. <https://doi.org/10.1021/cm301660n>
- [17] Onwudiwe, D.C.; Ajibade, P.A. Synthesis and Crystal Structure of Bis(N-Alkyl-N-Phenyl Dithiocarbamate)Mercury(II). *J. Chem. Crystallogr.* **2011**, *41*, 980–985. <https://doi.org/10.1007/s10870-011-0029-3>
- [18] de Faria Franca, E.; Oliveira, M.R.L.; Guilardi, S.; de Andrade, R.P.; Lindemann, R.H.; Amim, J.; Ellena, J.; De Bellis, V.M.; Rubinger, M.M.M. Preparation, Crystal Structure and Spectroscopic Characterization of Nickel(II) Complexes with Dithiocarbamate Derivated of Sulfonamides. *Polyhedron* **2006**, *25*, 2119–2126. <https://doi.org/10.1016/j.poly.2005.11.035>
- [19] Manoussakis, G.E.; Tsipis, C.A.; Christophides, A.G. Tris(Dialkyldiselenocarbamates) of Arsenic, Antimony, and Bismuth. *Inorg. Chem.* **1973**, *12*, 3015–3017. <https://doi.org/10.1021/ic50130a059>
- [20] Chen, D.; Lai, C.S.; Tiekink, E.R.T. Crystallographic Report: Tris(N,N-Dimethyldithiocarbamate)Arsenic(III) Dichloromethane Solvate. *Appl. Organomet. Chem.* **2003**, *17*, 813–814. <https://doi.org/10.1002/aoc.515> <https://doi.org/10.1002/aoc.515>
- [21] Ritsema, R. Speciation of Organotin and Organoarsenic in Water Samples. *Mikrochim. Acta* **1992**, *109*, 61–65. <https://doi.org/10.1007/BF01243211>
- [22] Adeyemi, J.O.; Onwudiwe, D.C.; Hosten, E.C. Organotin(IV) Complexes Derived from N-Ethyl-N-Phenyldithiocarbamate: Synthesis, Characterization and Thermal Studies. *J. Saudi Chem. Soc.* **2018**, *22*, 427–438. <https://doi.org/10.1016/j.jscs.2017.08.004>
- [23] Mahato, M.; Mukherji, S.; Van Hecke, K.; Harms, K.; Ghosh, A.; Nayek, H.P. Mononuclear Homoleptic Organotin(IV) Dithiocarbamates: Syntheses, Structures and Antimicrobial Activities. *J. Organomet. Chem.* **2017**, *853*, 27–34. <https://doi.org/10.1016/j.jorganchem.2017.10.027>
- [24] Adeyemi, J.O.; Onwudiwe, D.C.; Singh, M. Synthesis, Characterization, and Cytotoxicity Study of Organotin(IV) Complexes Involving Different Dithiocarbamate Groups. *J. Mol. Struct.* **2019**, *1179*, 366–375. <https://doi.org/10.1016/j.molstruc.2018.11.022>

- [25] Mihsen, H.H.; Shareef, N.K.; Alwazni, W.S. Synthesis, Characterization and Antibacterial Studies of Silver Complex of 3-Aminopropyltriethoxysilane. *Asian J. Chem.* **2018**, *30*, 1465. <https://doi.org/10.14233/ajchem.2018.21177>
- [26] Mihsen, H.H.; Shareef, N.K. Synthesis, Characterization of Mixed-Ligand Complexes Containing 2,2-Bipyridine and 3-Aminopropyltriethoxysilane. *J Phys Conf Ser* **2018**, *1032*, 012066. <https://doi.org/10.1088/1742-6596/1032/1/012066>
- [27] Hassan, Z.M.; Alattar, R.A.; Abass, S.K.; Mihsen, H.H.; Abbas, Z. F.; Hussain, K.A. Synthesis, Characterization and Biological Activity of Mixed Ligand (Imine of Benzidine and 1,10-Phenanthroline) Complexes with Fe(II), Co(II), Ni(II) and Cu(II) Ions. *Chem. Chem. Technol.* **2022**, *16*, 15–24. <https://doi.org/10.23939/chcht16.01.015>
- [28] Hartwell, S.K.; Grudpan, K.; Christian, G.D. Bead Injection with a Simple Flow-Injection System: An Economical Alternative for Trace Analysis. *Trends Anal. Chem.* **2004**, *23*, 619–623. <https://doi.org/10.1016/j.trac.2004.06.005>
- [29] Oliveira, M.R.L.; De Bellis, V.M. Preparation of Novel Cobalt(III) Complexes with Dithiocarbamates Derived from Sulfonamides. *Transit. Met. Chem.* **1999**, *24*, 127–130. <https://doi.org/10.1023/A:1006945923839>
- [30] Mihsen, H.H.; Abass, S.K.; Abass, A.K.; Hussain, K.A.; Abbas, Z.F. Template Synthesis of Sn(II), Sn(IV) and Co(II) Complexes via 3-Aminopropyltriethoxysilane and Salicylaldehyde and Evaluate Their Antibacterial Sensitivity. *Asian J. Chem.* **2018**, *30*, 2277. <https://doi.org/10.14233/ajchem.2018.21439>
- [31] Jamuna Rani, P.; Thirumaran, S.; Ciattini, S. Synthesis and Characterization of Ni(II) and Zn(II) Complexes of (furan-2-yl)methyl(2-(thiophen-2-yl)ethyl)dithiocarbamate (ftpedtc): X-ray Structures of [Zn(ftpedtc)2(py)] and [Zn(ftpedtc)Cl(1,10-phen)] *Spectrochim. Acta A Mol. Biomol. Spectrosc.* **2015**, *137*, 1164–1173. <http://dx.doi.org/10.1016/j.saa.2014.09.019>
- [32] Mohammad, A.; Varshney, C.; Nami, S.A.A. Synthesis, Characterization and Antifungal Activities of 3d-Transition Metal Complexes of 1-Acetyl piperazinyldithiocarbamate, M(acpdtc)<sub>2</sub>. *Spectrochim. Acta A Mol. Biomol. Spectrosc.* **2009**, *73*, 20–24. <https://doi.org/10.1016/j.saa.2009.01.005>
- [33] Geetha, N.; Thirumaran, S. Characterization Studies and Cyclic Voltammetry on Nickel (II) Amino Acid Dithiocarbamates with Triphenylphosphine in the Coordination Sphere. *J. Serbian Chem. Soc.* **2008**, *73*, 169–177. <https://doi.org/10.2298/JSC0802169G>
- [34] Chauhan, H.P.S.; Shaik, N.M. Synthetic, Spectral, Thermal and Antimicrobial Studies on Some Mixed 1,3-Dithia-2-Stannacyclopentane Derivatives with Dialkyldithiocarbamates. *J. Inorg. Biochem.* **2005**, *99*, 538–545. <https://doi.org/10.1016/j.jinorgbio.2004.10.031>
- [35] Nami, S.A.A.; Siddiqi, K.S. Convenient One-Pot Synthesis of Symmetrical Dithiocarbamates. *Synth. React. Inorg. Met. Chem.* **2004**, *34*, 1581–1590. <https://doi.org/10.1081/SIM-200026593>
- [36] Tweedy, B.G. Possible Mechanism for Reduction of Elemental Sulfur by *Monilinia fructicola*. In *Phytopathology*; 3340 PILOT KNOB ROAD, ST PAUL, MN 55121: Amer Phytopathological Soc, 1964; pp 910-914.
- [37] Mihsen, H. H.; Abass, S. K.; Hassan, Z. M.; Abass, A. K. Synthesis, Characterization and Antimicrobial Activities of Mixed Ligand Complexes of Fe (II), Co (II), Ni (II) and Cu (II) Ions Derived from Imine of Benzidine and o-phenylenediammine. *Iraqi J. Sci.* **2020**, *11*, 2762-2775. <https://doi.org/10.24996/ijcs.2020.61.11.2>

Received: January 15, 2022 / Revised: February 24, 2022 /

Accepted: May 24, 2022

### СИНТЕЗ, ХАРАКТЕРИСТИКА Й АНТИБАКТЕРІАЛЬНА АКТИВНІСТЬ КОМПЛЕКСІВ ІОНІВ Sn(II) ТА Sn(IV), ЩО МІСТЯТЬ N-АЛКІЛ-N- ФЕНІЛДИТИОКАРБАМАТНІ ЛІГАНДИ

**Анотація.** У цій роботі ліганди з донорними атомами S2, N-метил-N-фенілдитіокарбамат натрію [L1] та N-етил-N-фенілдитіокарбамат натрію [L2] одержано з дисульфід карбону за допомогою N-метиланіліну та N-етиланіліну, відповідно. Комплекси іонів Sn(II) та Sn(IV) з N-алкіл-N-фенілдитіокарбаматом одержано та охарактеризовано за допомогою CHNS елементного аналізу, інфрачервоної спектроскопії (FT-IR), <sup>1</sup>H ЯМР-спектроскопії, мас-спектроскопії, УФ-спектроскопії, вимірювання магнітної сприйнятливості та провідності. Аналітичні та спектральні дані показують, що стехіометрія для всіх комплексів становить 1 : 2 метал до ліганду. Спектральні дані підтверджують добру координацію дитіокарбаматного ліганду з металом через атоми сульфуру в дитіокарбаматному фрагменті. Вимірювання молярної провідності комплексів з використанням ДМФА як розчинника показало, що комплекси Sn(II) є неіонними, тоді як комплекси Sn(IV) є іонними. Ліганди L1 і L2 та їхні комплекси досліджено щодо бактерій *Staphylococcus aureus* і *Escherichia coli*.

**Ключові слова:** антибактеріальна активність, N-алкіл-N-фенілдитіокарбамат, комплекси стануму, спектральні дані.